Chalcogenide Letters Vol. 6, No. 4, April 2009, p. 163 - 170

OPTICAL, STRUCTURAL AND ELECTRICAL PROPERTIES OF THE NEW ABSORBER $Sn_2Sb_2S_5$ THIN FILMS

A. GASSOUMI*, M. KANZARI
Laboratoire de Photovoltaïque et Matériaux Semiconducteurs -ENIT BP 37, Le belvédère 1002-Tunis

Sulfosalt $Sn_2Sb_2S_5$ thin films have been deposited on glass substrates by vacuum evaporation method. The pressure during evaporation was maintained at 10^{-5} Torr. The films were annealed in air atmosphere in the temperatures range 100-250°C. The structural and the optical properties have been investigated relating the annealing temperature. Two optical direct transitions were found which decrease by increasing the annealing temperature. Absorption coefficients higher than 10^4 cm^{-1} were found. The X-ray diffraction analysis indicates that before and after air heat treatment only the $Sn_2Sb_2S_5$ phase is present. Furthermore, we found that the $Sn_2Sb_2S_5$ thin films exhibit N-type conductivity after annealing with lower resistivity. So, the new sulfosalt $Sn_2Sb_2S_5$ material is a good candidate for example for photovoltaic applications.

(Received March 25, 2009; accepted April 5, 2005)

Keywords: $Sn_2Sb_2S_5$, Thin films, Optical properties, X-ray diffraction, Surface morphology

1. Introduction

Studying the optical, structural and electrical properties of the sulfosalts materials has attracted great attention due to their interesting technological applications [1]. Sulfosalts belong to a class of complex sulfides with general formula of $A_mB_nX_p$, where A stands for metallic elements like Sn and Pb, B represents semi-metallic elements such as As, Sb, and Bi, and X can be either S or Se [2]. There are no works at our knowledge reported to the material $Sn_2Sb_2S_5$ in thin films form. This work deals with the effect of heat treatment in air atmosphere on structural, optical and electrical properties of the new absorber material $Sn_2Sb_2S_5$ in thin films form.

2. Experimental procedure

2.1. Synthesis of $Sn_2Sb_2S_5$

Stoichiometric amounts of 99.999% pure Sn, Sb, and S were used to prepare the initial ingot of $Sn_2Sb_2S_5$. The mixture was sealed in vacuum in a quartz tube. The quartz tube was heated slowly (10 °C/h). A complete homogenization could be obtained by keeping the melt at 600 °C for about 48 h. The tube was then cooled at a rate of 10 °C/h, so that cracking due to thermal expansion of the melt up on solidification was avoided. X-ray analysis of the powdered material (Fig.1) showed that only a homogenous $Sn_2Sb_2S_5$ phase was present in the ingot in comparison with the reference [3]. A crushed powder of this ingot was used as raw material for the thermal evaporation.

*Corresponding author: abdelaziz.gassoumi@gmail.com

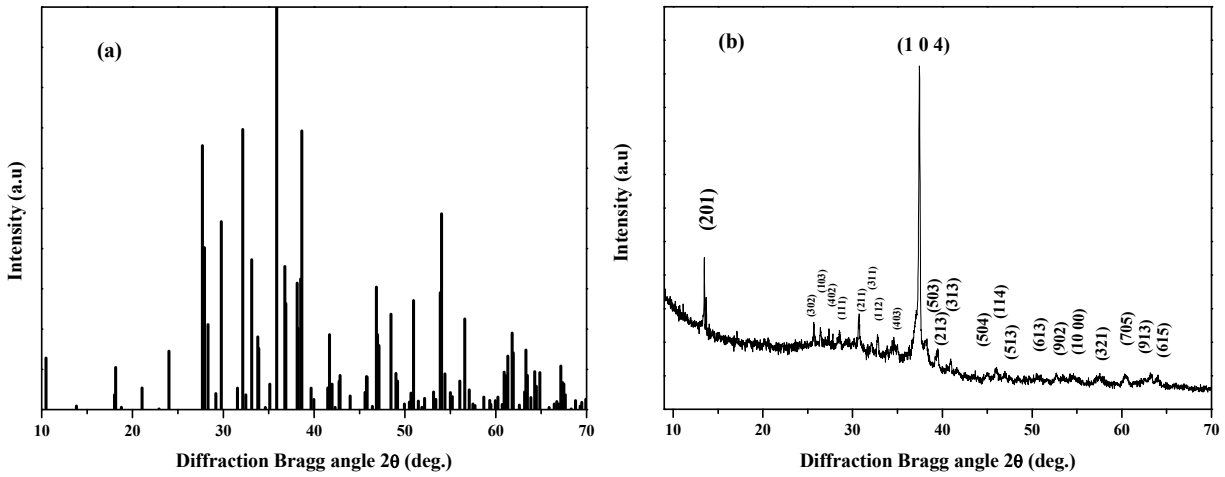

Fig.1:X-ray diffractogram of the $Sn_2Sb_2S_5$ powder (a): Ref [3] and (b): this work

2.2. Film preparation

$Sn_2Sb_2S_5$ films were deposited on un-heated glass substrates by thermal vacuum evaporation. The pressure during the evaporation was maintained at 10^{-5} Torr .A chromel-alumel thermocouple monitored the substrate temperature. The as-deposited $Sn_2Sb_2S_5$ films were thermally annealed for 1 hour under air atmospheric in the temperature range 100-250°C with a step of 50°C.

2.3. Characterization of the films

The structural properties were determined by X-ray diffraction (XRD) using cobalt $Co_{K\alpha 1}$ radiation (λ=0.1789 nm). Optical transmittance and reflectance were measured at normal incidence with a UV–visible–NIR Shimadzu 3100S spectrophotometer in the wavelength range 300–1800 nm. The film thicknesses were calculated from the positions of the interference maxima and minima in the reflectance spectra using a standard method [4]. The film thicknesses were found to be in the range 292-423 nm. The surface morphology and roughness of the films were examined means of atomic force microscopy (AFM) type Vecco model D3100. The hot probe method measurements were carried out in order to determine the conduction type of the samples.

3. Results and discussion

3.1. Structural and morphological properties

Fig. 2 shows the XRD patterns of the $Sn_2Sb_2S_5$ thin films before and after air heat treatment. As a surprising, the as-deposited $Sn_2Sb_2S_5$ film is crystallized in spite of the low substrate temperature (30 °C). Because in general semiconducting or dielectric materials deposited by thermal evaporation method present a dominant amorphous component the $SnSb_2S_5$ shows an exceptional case since it is deposited in crystallize form at low substrate temperature. Only the strong principal diffraction line related to the $Sn_2Sb_2S_5$ phase appeared before annealing. After annealing, the strong principal diffraction line is accompanied with a minor secondary diffraction line which also associated to the $Sn_2Sb_2S_5$ phase.
The crystallite size (*D*) is calculated using the well-known Scherrer's formula [5]:

$$D = \frac{0.9\lambda}{\beta \cos\theta} \quad (1)$$

where β is the value of the full width at half maximum (FWHM).
The average grain sizes of the layers were calculated using the principal diffraction line which evaluated to be in the range (204-212) Å as shown in figure 3. It is clear that the heat treatment in air atmosphere does not affect significantly the grain sizes of the $Sn_2Sb_2S_5$ thin films.

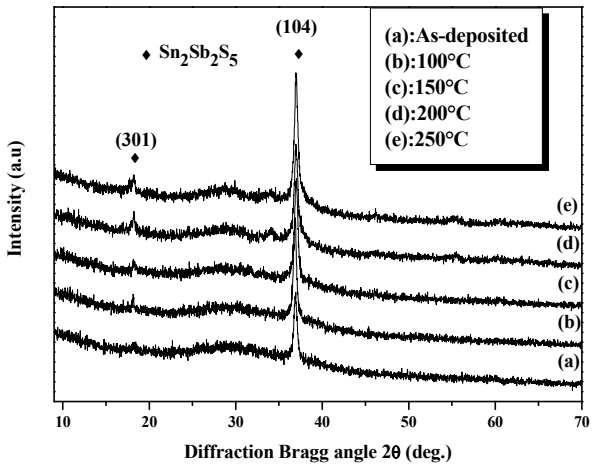

Fig.2. X-ray diffraction patterns of as-deposited and annealed $Sn_2Sb_2S_5$ thin films at various annealing temperatures

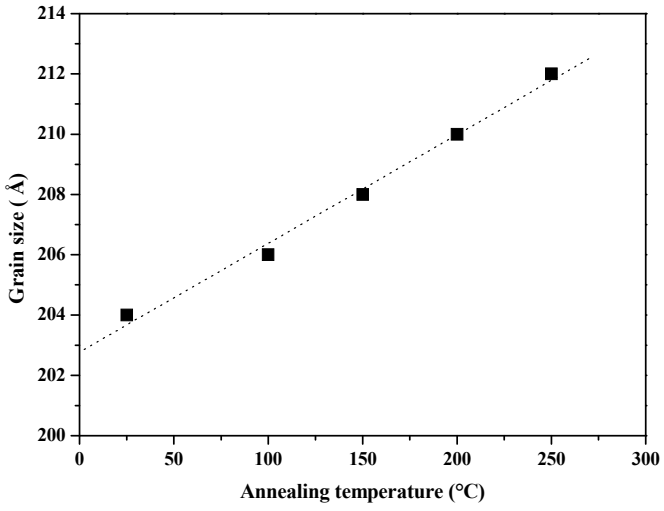

Fig.3. Grain size versus the annealing temperature of the polycrystalline $Sn_2Sb_2S_5$ thin films.

In order to clarify the role of the thermal annealing effect, we studied surface morphologies of the $Sn_2Sb_2S_5$ films by Atomic Force Microscopy (AFM). Fig. 4 shows their surface morphologies analyzed by AFM. It should be easily found that a low rough surface was obtained independently of the annealing temperature with average roughness of 7.6 nm. It seems to be extraordinarily low, since the average thickness of the films is 350 nm.

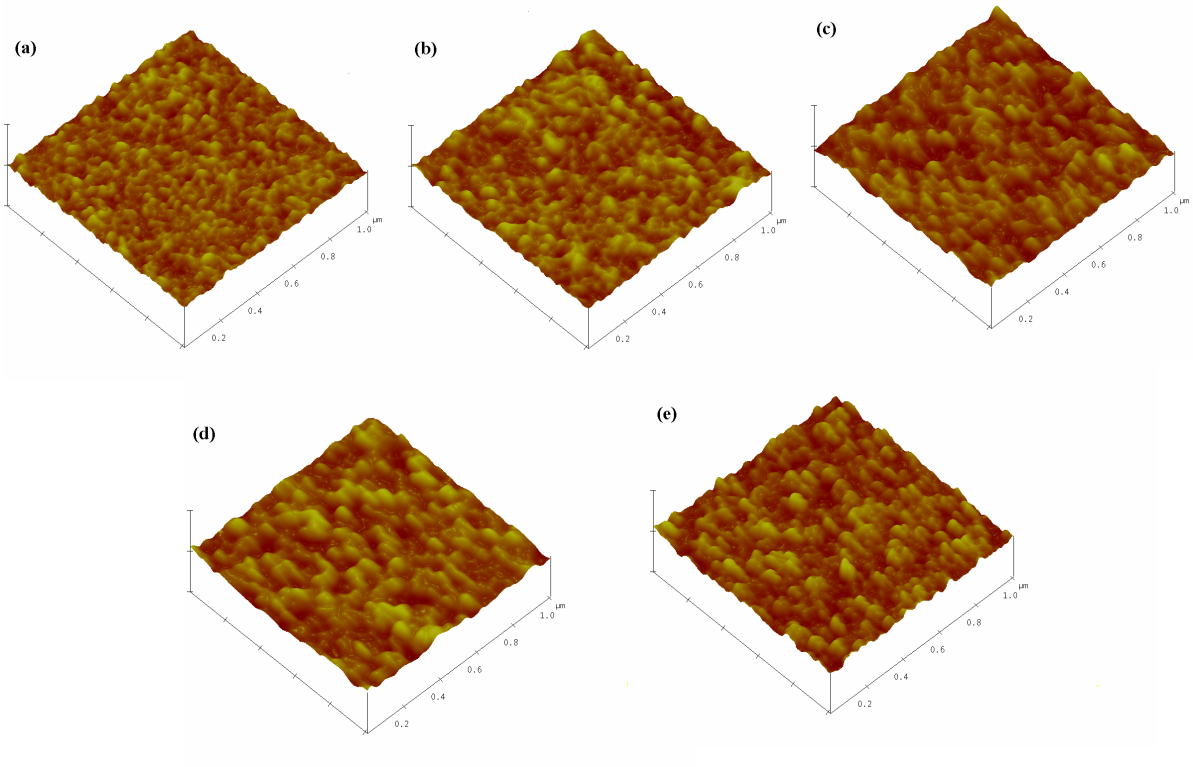

Fig.4. 3D AFM images of $Sn_2Sb_2S_5$ films surface: (a) As-deposited,(b)100°C,(c)150°C, (d)200°C and (e)250°C.

3.2. Optical properties

3.2.1. Optical transmittance and reflectance spectra

The optical properties of the $Sn_2Sb_2S_5$ thin films were studied by measuring at normal incidence both transmittance (T) and reflectance (R) spectra in the spectral range 300–1800 nm. Figure 5 shows the transmittance and the reflectance spectra respectively before and after annealing. All the spectra reveal very pronounced interference effects in the transparency region 900-1800 nm with sharp fall of transmittance at the band edge. The transmittance values were in the range 55-60% in the transparency region for the samples before and after air heat treatment. In addition the values of the reflectance for all the samples were in the range 40-45% which means that there is no absorption occurs in the spectral range 900-1800 nm.

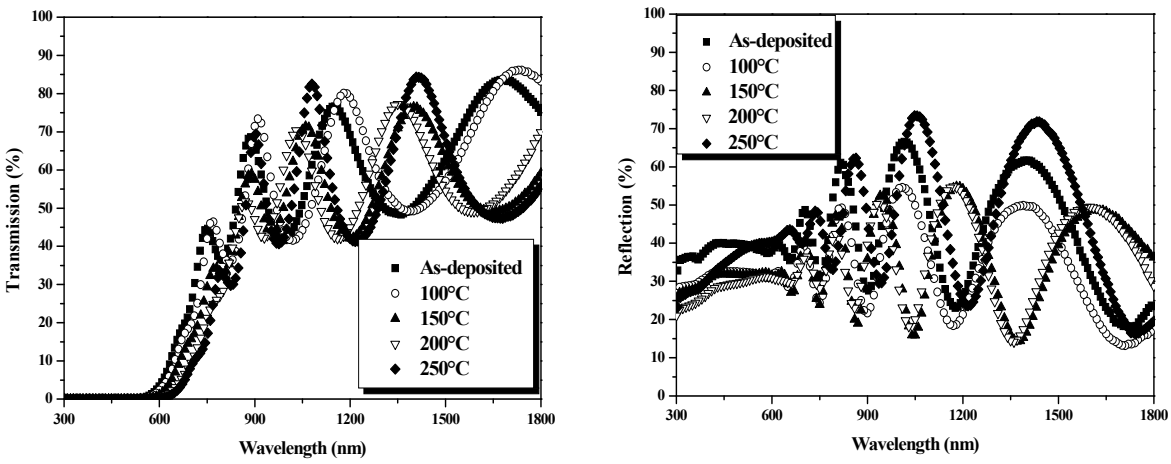

Fig.5: Transmittance (a) and reflectance (b) spectra of $Sn_2Sb_2S_5$ thin films at various annealing temperatures .

3.2.2. Values of the refractive indices

The values of the refractive indices (*n*) of the $Sn_2Sb_2S_5$ films were calculated approximately from the method described in [6] .Figure 6 shows the refractive index, n, of the $Sn_2Sb_2S_5$ films as a function of wavelength for the different annealing temperatures. The refractive index increases by increasing the annealing temperature from 2.62 to 2.8. Therefore we think that antimony element is the main responsible for the increase of the refractive index by increasing the annealing temperature. Indeed, it has been shown [7, 8] that after annealing temperature materials which contain antimony compound present an opaque aspect with high refractive indices.

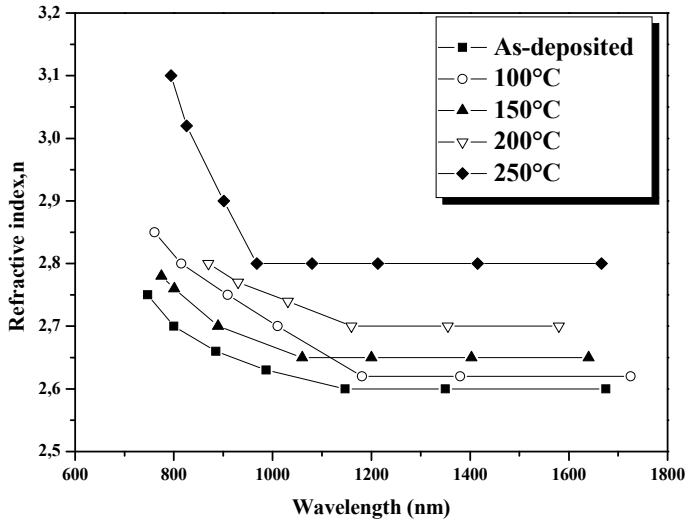

Fig.6: Refractive index n versus the wavelength for $Sn_2Sb_2S_5$ thin films at various annealing temperatures.

3.2.3. Absorption coefficients

To calculate the absorption coefficient $\alpha(h\upsilon)$, the following relationship was used [9]:

$$\alpha = \frac{1}{d}\ln\left[\frac{(1-R)^2}{T}\right] \tag{2}$$

Where d is the film thickness, and R and T are the reflection and transmission coefficient, respectively. Figure 7 shows the dependence of the absorption coefficient on photon energy for the $Sn_2Sb_2S_5$ films. It can be seen that all the $Sn_2Sb_2S_5$ films have relatively high absorption coefficients, higher than 10^4 cm^{-1} in the visible and the near-IR spectral region. This result is very important because the spectral dependence of the absorption coefficient is one of the important factors which affect the solar conversion efficiency.

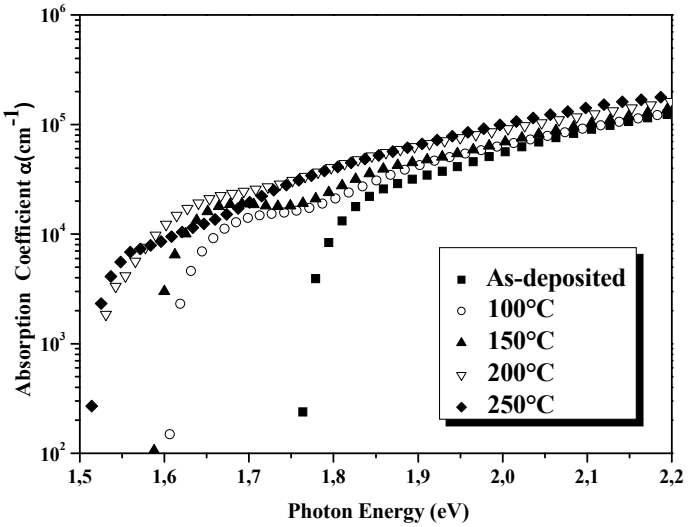

Fig.7: Absorption coefficient of the $Sn_2Sb_2S_5$ thin films for several annealing temperatures.

3.2.4. Energy gaps

The absorption coefficient α is related to the energy gap Eg according to the equation [10]:

$$\alpha h\nu = A\left(h\nu - \mathrm{Eg}\right)^n \tag{3}$$

where A is a constant, h is the Planck constant and n is equal to ½ for a direct gap and 2 for an indirect gap semiconductor. The band gap value Eg was determined by extrapolating the straight section of the $(\alpha h\upsilon)^2$ vs. $h\nu$ curve to the horizontal photon energy axis (Fig.8). Two direct band gaps corresponding to the energy gaps Eg_1 and Eg_2 were found for each sample. The energy gaps values Eg_1 are estimated to be in the range 1.52–1.78 eV (Fig.9) which corresponds to the valence band-conduction band transition. It was also found that Eg_1 decreases with increasing the annealing temperature. The transition with Eg_2 in the range 1.80-1.96 eV is probably associated with valence band spilling under the influence of the crystal field of lattice (Δ_{CF}) as observed in several materials [11,12].

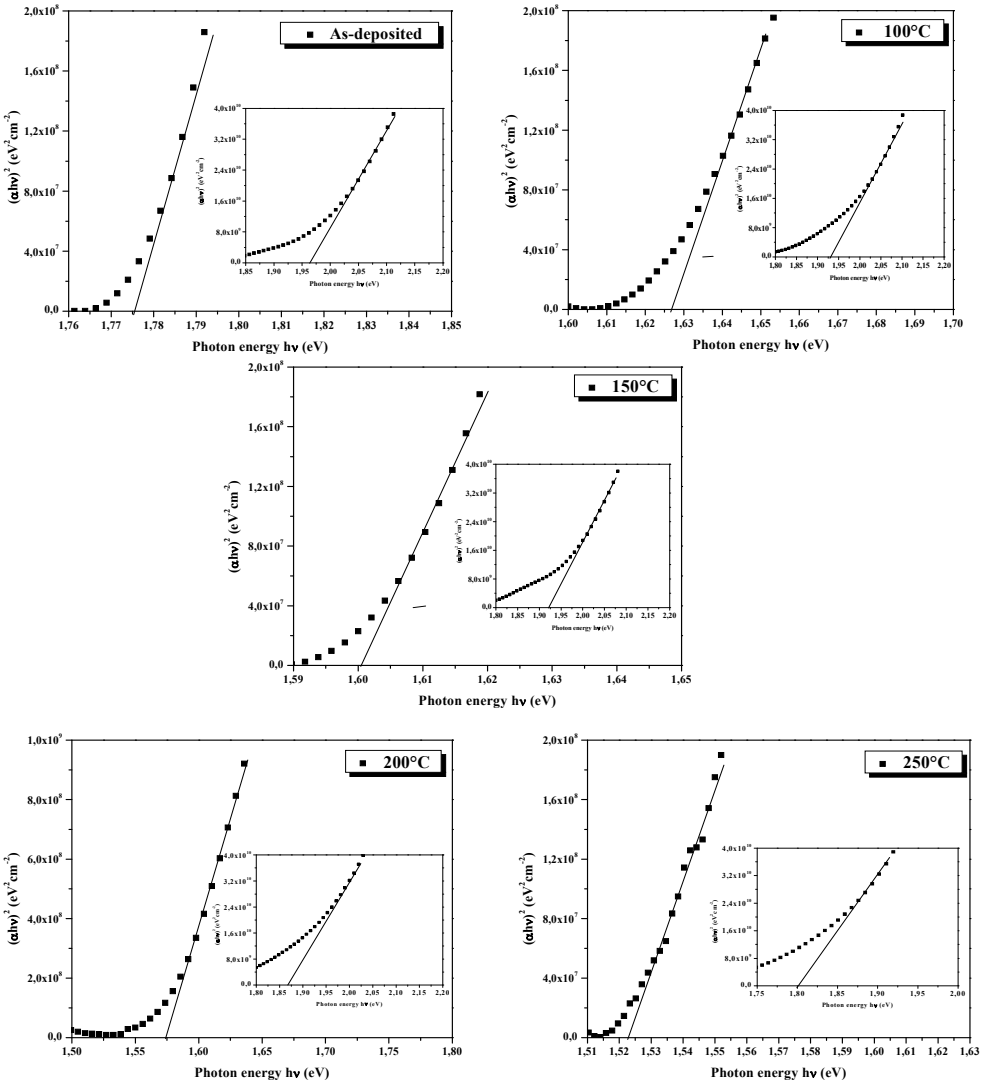

Fig.8: Plots of $(\alpha h\upsilon)^2$ versus $h\upsilon$ for the $Sn_2Sb_2S_5$ layers for various annealing temperatures.

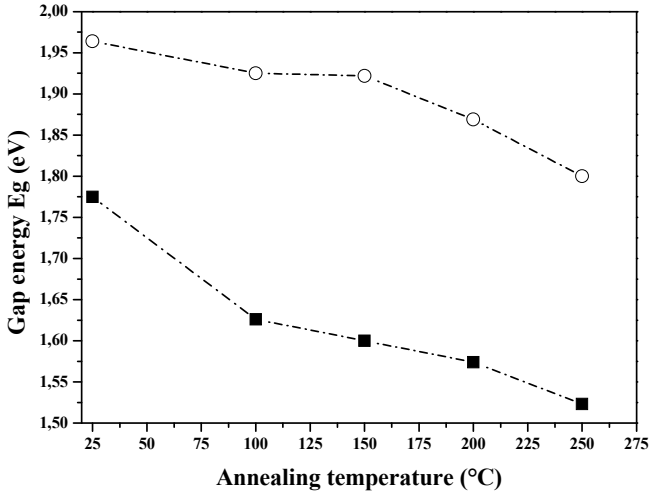

Fig.9: Band gap energies Eg_1 and Eg_2 dependence of the annealing temperature of the $Sn_2Sb_2S_5$ thin films.

3.3. Electrical properties

Besides the optical properties, the electrical properties are also an important aspect of the performance of $Sn_2Sb_2S_5$ thin films. Before annealing, the as-deposited $Sn_2Sb_2S_5$ samples are highly compensated and no significantly conduction type is observed. After annealing in air all the films presented low electrical resistivity with low N-type conductivity. The resistivity decreases after annealing at 100°C until $35.10^{-4}\Omega$cm and increases to 14.10^{-3} Ωcm when the films were annealed at 250°C. The origin of the N type conductivity after air annealing is not understood at this state since no works were reported for this material in thin films forms. However we suggest that after the annealing in air introduces a donor level which can explain the origin of the N-type conductivity. In this case the effect of the oxygen incorporation is not understood since any oxide phases were detected in the samples.

4. Conclusions

This study deals with the new absorber $Sn_2Sb_2S_5$ material in thin film form. $Sn_2Sb_2S_5$ films were deposited by thermal evaporation method on glass substrates. The $Sn_2Sb_2S_5$ powder of this ingot was previously synthesized by Bridgman method and used as raw material for the thermal evaporation. The as-deposited films were annealed in air atmosphere in the temperature range 50-250°C The as-deposited films are crystallized in nature and no great effect in structural properties after annealing is found.. Absorption coefficients higher than 10^4 cm^{-1} were found. Two optical direct transitions were found which decrease with increasing the annealing temperature. The first band gap in the range 1.52–1.78 eV is attributed to the transition valence band to conduction band. The second energy band gap in the range 1.80-1.96 eV corresponds probably to the valence band spilling under the influence of the crystal field of lattice.We found that the $Sn_2Sb_2S_5$ thin films exhibit N-type conductivity after annealing with lower resistivity.

References

[1] H. Dittrich, A. Bieniok, U.Brendel, M. Grodzicki, D. Topa, Thin Solid Films **515**, 5745 (2007).
[2] Galina N. Kryukovaa, Matthias Heuerb, Gerald Wagnerb, Thomas Doeringb and Klaus Bente Journal of Solid State Chemistry **178,** 376 (2005).
[3] Smith, P.P.K., Hyde, B.G., Acta Crystallogr., Sec. C, **39**, 1498 (1983).
[4] K. L. CHOPRA, "Thin Film Phenomena" (McGraw-Hill, New York, 1969) p. 721.
[5] S.F. Bartram, Handbook of X-Rays, edited by E.F. Kaelebe (McGraw-Hill, New York, 1967), Chap.17.
[6] M. Zribi, M. Kanzari , B. Rezig Materials Letters **60**, 98 (2006).
[7] A.Gassoumi, M. Kanzari and B. Rezig .Eur. Phys. J. Appl. Phys. **41**, 91 (2008).
[8] A. Rabhi, M. Kanzari M, B. Rezig, Materials Letters **62**, 3576 (2008).
[9] T.S. Moss, Optical Properties of Semiconductors, Butterworth, London, 1959.
[10] E.A. Davis, N.F. Mott, Philipp. Mag. **22**, 903 (1970).
[11] A.H.Ammar,A.M.Farid,M.A.M.Seyam ,Vaccum **66**, 27 (2002) -38.
[12] I.V.Bodnar,I..T.Bodnar,I.A.Victorov,V.F.Gremenok,M.Leon ,Moldavian Journal of the Physical Sciences, Vol.5, N3-4,2006.